Turbulent diffusion in protoplanetary discs: the effect of an imposed magnetic field

A. Johansen,[1]★ H. Klahr[1] and A. J. Mee[2]

[1]*Max-Planck-Institut für Astronomie, Königstuhl 17, 69117 Heidelberg, Germany*
[2]*School of Mathematics and Statistics, University of Newcastle upon Tyne, Newcastle NE1 7RU*

ABSTRACT

We study the effect of an imposed vertical magnetic field on the turbulent mass diffusion properties of magnetorotational turbulence in protoplanetary discs. It is well-known that the effective viscosity generated by the turbulence depends strongly on the magnitude of such an external field. In this Letter we show that the turbulent diffusion of the flow also changes, but that the diffusion coefficient does not rise with increasing vertical field as fast as the viscosity does. The vertical Schmidt number, i.e. the ratio between viscosity and vertical diffusion, can be close to 20 for high field magnitudes, whereas the radial Schmidt number is increased from below unity to around 3.5. Our results may have consequences for the interpretation of observations of dust in protoplanetary discs and for chemical evolution modelling of these discs.

Key words: accretion, accretion discs – diffusion – MHD – turbulence – planetary systems: formation – planetary systems: protoplanetary discs.

1 INTRODUCTION

Planets form out of micrometre-sized dust grains that are embedded in the gas in protoplanetary discs [see Dominik et al. (2006) for a recent review]. The observed infrared radiation from protoplanetary discs comes primarily from micron-sized grains, although observations at longer wavelengths show that some discs have large populations of grains with sizes up to millimetres and centimetres (e.g. Rodmann et al. 2006). Turbulent motions in the gas play a big role in the dynamics of chemical species and solids, at least as long as the solids are smaller than a few tens of metres. Thus an understanding of how dust grains and chemical species move under the influence of turbulence is vital for our understanding of the physical processes that take place in protoplanetary discs and the observational consequences (Ilgner et al. 2004; Ilgner & Nelson 2006; Willacy et al. 2006; Dullemond, Apai & Walch 2006; Semenov, Wiebe & Henning 2006).

Turbulence has a number of effects on the embedded dust grains. Larger grains (rocks and boulders) can be trapped in the turbulent flow due to their marginal coupling to the gas (Barge & Sommeria 1995), whereas smaller grains feel the effect of the turbulence as a combination of diffusion and simple advection. Any bulk motion of the gas, e.g. turbulent motion with a turnover time that is longer than the time-scale that is considered or even a radial accretion flow, leads to an advective transport of the dust grains rather than

★E-mail: johansen@mpia.de

diffusion. The turbulent transport acts as diffusion only when the considered time-scale is longer than the eddy turnover time. The turbulent diffusion coefficient of the grains, $D_t = \delta c_s^2 \, \Omega_0^{-1}$, is often assumed to be equal to the turbulent viscosity of the gas flow, $\nu_t = \alpha c_s^2 \, \Omega_0^{-1}$. Here a non-dimensionalization with sound speed c_s and Keplerian frequency Ω_0 is used (Shakura & Sunyaev 1973). The Schmidt number, a measure of the relative strength of turbulent viscosity and turbulent diffusion, is defined as the ratio $\mathrm{Sc} = \nu_t/D_t = \alpha/\delta$. Several recent works have measured the turbulent diffusion coefficient directly from numerical simulations of magnetorotational turbulence (Balbus & Hawley 1991). The simulations by Johansen & Klahr (2005, hereafter JK05) yielded a Schmidt number that is around unity for radial diffusion, whereas Carballido, Stone & Pringle (2005, hereafter CSP05) found a value as high as 10. The vertical Schmidt number, measured by JK05, Turner et al. (2006) and Fromang & Papaloizou (2006), gives more consistently a number between 1 and 3. Here it is worthy of note that Turner et al. (2006) consider stratified discs, and Fromang & Papaloizou (2006) even include the effect of a magnetically dead zone without turbulence around the mid-plane (Gammie 1996; Fleming & Stone 2003).

This Letter addresses the discrepancy between the diffusion properties of turbulence in protoplanetary discs reported in the literature. We show that a vertical imposed magnetic field affects the diffusion coefficient strongly. It is known that a net vertical field component leads to turbulence with a stronger angular momentum transport (Hawley, Gammie & Balbus 1995). We perform computer simulations of magnetorotational turbulence for various values of the

vertical field and find that turbulent diffusion does not increase as much as the viscosity increases. Thus the ratio between viscous stress and diffusivity, i.e. the Schmidt number, also increases with the magnitude of the external field. As a result we are able to give a possible explanation for the discrepancy in the radial Schmidt numbers found in the literature.

2 SOURCES OF AN EXTERNAL MAGNETIC FIELD

The properties of any external magnetic field threading protoplanetary discs are not well-known. Close to the central object there is an interaction with the possibly dipolar or maybe quadrupolar magnetic field of the young stellar object. Also the occurrence of jet phenomena indicates that at least for the originating zone of the jet, e.g. a few protostar radii, there should be a large-scale vertical magnetic field (e.g. Fendt & Elstner 1999; Vlemmings, Diamond & Imai 2006). However, at larger orbital distances relevant for planet formation, it is not obvious what the global field configuration should look like.

To get some physical insight into the role of an external magnetic field in the dynamics of protoplanetary discs, we do here some rough estimations for two cases, either that the field originates in the central object, or that it comes from the molecular cloud core out of which the disc formed.

2.1 Protostar

The dipolar field of the central protostar dominates the gas pressure of the disc until a certain inner disc radius $R_{\rm in}$. This is typically a few times the protostellar radius (Camenzind 1990; Königl 1991; Shu et al. 1994). Beyond $R_{\rm in}$ the interaction between the dipole field and the accretion disc is strongly unstable and leads to an opening up of the protostellar dipole field lines (Miller & Stone 1997; Fendt & Elstner 2000; Küker, Henning & Rüdiger 2003). Even if the protostar could retain its dipolar field at larger orbital radii, the magnetic pressure exerted by the field lines would fall so quickly with orbital radius $[B_z^2(r) \propto r^{-6}]$ that it would be completely unimportant at several au from the protostar where the gas planets are believed to form.

2.2 Molecular cloud

In molecular cloud cores the magnetic field, $B_{\rm cloud}$, can be as large as $\sim 100\,\mu{\rm G}$ (Bourke et al. 2001). The gas pressure in the disc can be written as $P = c_s^2\,\rho$, where c_s is the sound speed and ρ is the gas density. The mid-plane density of an exponentially stratified disc with scaleheight H depends on the column density Σ as $\rho = \Sigma/(\sqrt{2\pi}H)$. The scaleheight to radius ratio H/r, which also corresponds to the ratio of local sound speed to Keplerian speed $v_{\rm K}$, can be used to rewrite the gas pressure at the mid-plane of the disc as

$$P = \left(\frac{H}{r}\right)^2 v_{\rm K}^2 \frac{\Sigma(r)}{\sqrt{2\pi}(H/r)r} = \frac{H}{r}\frac{GM_\star}{\sqrt{2\pi}}\frac{\Sigma(r)}{r^2}. \tag{1}$$

The plasma beta of the external magnetic field is defined as the ratio between gas pressure and magnetic pressure $\beta = P/P_{\rm mag}$. One can write the following scaling for the plasma beta $\beta_{\rm cloud}$ due to the magnetic field from the molecular cloud:

$$\beta_{\rm cloud} = 5.9 \times 10^7 \left(\frac{H/r}{0.1}\right)\left(\frac{M_\star}{{\rm M}_\odot}\right)\left(\frac{B_{\rm cloud}}{\mu{\rm G}}\right)^{-2}$$

$$\times \left(\frac{\Sigma}{1\,{\rm g\,cm}^{-2}}\right)\left(\frac{r}{100\,{\rm au}}\right)^{-2}. \tag{2}$$

Here $\beta_{\rm cloud}$ has a falling trend with r because the low gas density in the outer part of the disc makes the magnetic pressure more important there. For a sufficiently strong cloud field, the plasma beta could be relatively low at a disc radius of several hundred astronomical units.

3 SIMULATIONS

We simulate a protoplanetary disc in the shearing sheet approximation (e.g. Goldreich & Tremaine 1978; Brandenburg et al. 1995; Hawley et al. 1995). Here a local coordinate frame corotating with the disc with the Keplerian rotation frequency Ω_0 at a distance r_0 from the central source of gravity is considered. The coordinate system is oriented so that x points radially away from the central object, y points in the azimuthal direction parallel to the the Keplerian flow, and z points normal to the disc along the Keplerian rotation vector $\boldsymbol{\Omega}_0$. Numerical calculations are performed using the Pencil Code [a finite difference code that uses sixth-order symmetric space derivatives and a third-order time-stepping scheme – see Brandenburg (2003)].

3.1 Gas

Considering the velocity field $\boldsymbol{u}$ relative to the Keplerian flow $u_y^{(0)} = -(3/2)\,\Omega_0\,x$, the equation of motion of the gas is

$$\frac{\partial \boldsymbol{u}}{\partial t} + (\boldsymbol{u}\cdot\nabla)\boldsymbol{u} + u_y^{(0)}\frac{\partial \boldsymbol{u}}{\partial y} = \boldsymbol{f}(\boldsymbol{u}) - c_s^2 \nabla\ln\rho$$

$$+ \frac{1}{\rho}\boldsymbol{J}\times(\boldsymbol{B} + B_0\hat{z}) + \boldsymbol{f}_\nu. \tag{3}$$

The left-hand side of equation (3) contains terms both for the advection by the velocity relative to the Keplerian flow and for the advection by the Keplerian flow itself. The terms on the right-hand side are the modified Coriolis force,

$$\boldsymbol{f}(\boldsymbol{u}) = \begin{pmatrix} 2\Omega_0 u_y \\ -\frac{1}{2}\Omega_0 u_x \\ 0 \end{pmatrix}, \tag{4}$$

which takes into account that the Keplerian velocity profile is advected with any radial motion, the force due to the isothermal pressure gradient with a constant sound speed c_s, the Lorentz force (including the contribution from an imposed vertical field of strength B_0) and the viscous force $\boldsymbol{f}_\nu$ that is used to stabilize the numerical scheme. The viscosity term is a combination of sixth-order hyperviscosity and a localized shock capturing viscosity. The use of hyperviscosity, hyperdiffusion and hyperresistivity is explained in JK05. For the shock viscosity, where extra bulk viscosity is added in regions of flow convergence, we refer to Haugen, Brandenburg & Mee (2004) for a detailed description.

The evolution of the mass density is solved for in the continuity equation

$$\frac{\partial\rho}{\partial t} + \boldsymbol{u}\cdot\nabla\rho + u_y^{(0)}\frac{\partial\rho}{\partial y} = -\rho\nabla\cdot\boldsymbol{u} + f_{\rm D}, \tag{5}$$

where $f_{\rm D}$ is a combination of sixth-order hyperdiffusion and shock diffusion. The magnetic field evolves by the induction equation which we write in terms of the magnetic vector potential $\boldsymbol{A}$,

$$\frac{\partial\boldsymbol{A}}{\partial t} + u_y^{(0)}\frac{\partial\boldsymbol{A}}{\partial y} = \frac{3}{2}\Omega_0 A_y\hat{x} + \boldsymbol{u}\times(\boldsymbol{B} + B_0\hat{z}) + \boldsymbol{f}_\eta. \tag{6}$$

Again we use sixth-order hyperresistivity and shock resistivity, through the function $\boldsymbol{f}_\eta$, in regions of strong flow convergence. The value of B_0 sets the strength of an external vertical magnetic field.

Table 1. Measured turbulent viscosity and diffusion coefficients.

Run	$L_x \times L_y \times L_z$	B_0	β	α	Ma_x	Ma_y	Ma_z	δ_x	Sc_x	δ_z	Sc_z
A	$1.32 \times 1.32 \times 1.32$	0.00	∞	0.0028 ± 0.0004	0.053	0.053	0.041	0.0031	0.90	0.0016	1.75
B	–	0.01	20000	0.0078 ± 0.0015	0.079	0.092	0.064	0.0058	1.34	0.0031	2.52
C	–	0.03	2222	0.0367 ± 0.0142	0.197	0.185	0.140	0.0225	1.63	0.0092	3.99
D	–	0.05	800	0.1811 ± 0.0773	0.416	0.300	0.181	0.0574	3.16	0.0123	14.72
E	–	0.07	408	0.5529 ± 0.0964	0.761	0.421	0.330	0.1984	2.79	0.0300	18.43
A4	$1.00 \times 4.00 \times 1.00$	0.00	∞	0.0015 ± 0.0002	0.055	0.036	0.031	0.0017	0.88	0.0009	1.71
B4	–	0.01	20000	0.0038 ± 0.0009	0.079	0.057	0.052	0.0038	1.00	0.0024	1.58
C4	–	0.03	2222	0.0414 ± 0.0176	0.206	0.182	0.134	0.0177	2.34	0.0078	5.31
D4	–	0.05	800	0.0793 ± 0.0371	0.279	0.239	0.179	0.0268	2.96	0.0091	8.71
E4	–	0.07	408	0.1242 ± 0.0694	0.366	0.291	0.221	0.0356	3.49	0.0121	10.26

3.2 Dust particles

The turbulent diffusion coefficient D_t of the flow is measured by letting dust grains settle to the mid-plane of the turbulent disc. The dust layer is represented as individual particles each with a position $\boldsymbol{x}^{(i)}$ and velocity vector $\boldsymbol{v}^{(i)}$ (measured relative to the Keplerian velocity $u_y^{(0)}\hat{\boldsymbol{y}}$). The gas acts on a dust particle through a drag force that is proportional to but in the opposite direction from the difference between the velocity of the particle and the local gas velocity. The dust grains do not interact mutually and do not have any feedback on the gas. The equation of motion of the dust particles is

$$\frac{\mathrm{d}\boldsymbol{v}^{(i)}}{\mathrm{d}t} = \boldsymbol{f}\left(\boldsymbol{v}^{(i)}\right) - \frac{1}{\tau_f}\left(\boldsymbol{v}^{(i)} - \boldsymbol{u}\right) + \boldsymbol{g}, \tag{7}$$

where the modified Coriolis force $\boldsymbol{f}$ is defined in equation (4), τ_f is the friction time and $\boldsymbol{g}$ is an imposed gravitational field (see below). We assume in the following that τ_f is constant and thus independent of the relative velocity between the grain and the surrounding gas. In protoplanetary discs this is a valid assumption for sufficiently small dust grains (Weidenschilling 1977). We use a value of $\Omega_0\,\tau_f = 0.01$ which is small enough that the diffusion coefficient should not differ significantly from that of a passive scalar (which can be seen as a dust grain in the limit of a vanishingly small friction time). This value is also large enough that the computational time-step is set by the Courant criterion for the gas and not by the friction force in the dust equations.

The particles change positions according to the dynamical equation

$$\frac{\mathrm{d}\boldsymbol{x}^{(i)}}{\mathrm{d}t} = \boldsymbol{v}^{(i)} + u_y^{(0)}\hat{\boldsymbol{y}}. \tag{8}$$

Under the effect of a special gravity field acting on the dust only, $\boldsymbol{g}$ in equation (7), the particles fall either to the horizontal mid-plane of the disc, in the case of a vertical gravity field $\boldsymbol{g} = g_z(z)\hat{\boldsymbol{z}}$, or to a vertical 'mid-plane' in the case of a radial gravity field $\boldsymbol{g} = g_x(x)\hat{\boldsymbol{x}}$. We use a sinusoidal expression $g_i = -g_0 \sin(k_i x_i)$ with a wavelength that is equal to the size of the simulation box. In the equilibrium state, the sedimentation is balanced by the turbulent diffusion away from the mid-plane, and the dust number density n, for the case of a vertical gravity field, is given by (see JK05)

$$\ln n(z) = \ln n_1 + \frac{\tau_f g_0}{k_z D_z^{(t)}}\cos(k_z z), \tag{9}$$

where n_1 is an integration constant. The equivalent expression for the radial gravity case is found simply by replacing z by x in equation (9).

We run simulations with different values of the external magnetic field strength B_0 between 0 and 0.07, corresponding to a β ranging from infinity down to approximately 400. Our computational unit of velocity is the constant sound speed c_s, length is in units of the disc scaleheight H, and density is measured in units of mean gas density ρ_0. In these units the turbulent viscosity and the turbulent diffusion coefficient, ν_t and D_t, are numerically equal to the dimensionless coefficients α and δ. The unit of the magnetic field is then $[B] = c_s\sqrt{\mu_0\rho_0}$ and is chosen such that $\mu_0 = 1$. For each value of B_0 we run one simulation with a vertical and one simulation with a radial gravitational field on the dust particles. The diffusion coefficients δ_x and δ_z are found by fitting a cosine function to the logarithmic dust density. From the amplitude we then determine the diffusion coefficient using equation (9). The run parameters and the results are shown in Table 1. Two simulation box sizes are considered, a square box with a side length of 1.32 and an elongated box with $(L_x, L_y, L_z) = (1.0, 4.0, 1.0)$ (similar to the setup of Sano et al. 2004). For the first case we use a resolution of 64^3 grid points and 1 000 000 dust particles. Simulations with 128^3 grid points were done by JK05 and showed only small differences from the 64^3 simulations in the measured Schmidt numbers. Each model is run for 20 local orbits, i.e. $20 \times 2\pi\Omega_0^{-1}$, of the disc. The runs with an elongated box are done with $64 \times 256 \times 64$ grid points and 4 000 000 dust particles.

4 RESULTS

For each value of the imposed magnetic field we have measured the α-value from the Reynolds and Maxwell stress tensors (see Table 1). The α-value grows approximately exponentially with B_0. An α-value close to unity can be reached already for $B_0 = 0.07$ (corresponding to $\beta \simeq 400$). A similar investigation into the dependence of α on an imposed vertical field was undertaken by Hawley et al. (1995). Comparing with Table 1 in that work, one sees that there is a relatively good agreement between those results and ours. Magnetorotational instability (MRI) with an imposed vertical field develops into a 'channel' solution (Hawley & Balbus 1992; Goodman & Xu 1994; Steinacker & Henning 2001), characterized by the transfer of the most unstable MRI mode to the largest scale of the simulation box and the subsequent decay of this large-scale mode (Sano & Inutsuka 2001). Sufficiently strong vertical fields can even cause stratified discs to break up altogether (Miller & Stone 2000). The creation and destruction of the unstable channel solution give significant temporal fluctuations in the measured stresses, evident in the standard deviation of the turbulent viscosity in Table 1 (see also fig. 1 of Sano & Inutsuka 2001).

For measuring the turbulent diffusion coefficient we consider the logarithmic number density of the dust particles averaged from 10 to 20 orbits. We have chosen to calculate the diffusion coefficient directly from this average state, rather than calculating it from the

instantaneous dust density at a given time t, because large-scale advection flow only works as diffusion when averaged over sufficiently long times. The average dust density is found to be in excellent agreement with the cosine distribution of equation (9) with a deviation from a perfect cosine of less than 5 per cent for all simulations. Thus diffusion is a good description of the turbulent transport over long time-scales. This is partly due to the fact that we consider diffusion at the largest scale of the flow, i.e. at a scale that is similar to or larger than the energy injection scale of the MRI. Diffusion over length-scales that are smaller than the energy injection scale should be weaker, because dust density concentrations at small length-scales are not stretched by the full velocity amplitude of the larger scales, but only by the velocity difference that the larger scales exert over the much narrower dust concentration. The exp (cos) equilibrium state for the dust density, however, has almost all of its power at the largest scale of the simulation box, so any scale-dependence of the diffusion coefficient should not have any influence on the equilibrium state (the fact that the logarithmic dust density in the equilibrium state is a cosine supports this).

The measured turbulent diffusion coefficients are written in Table 1. It is evident that the turbulent diffusion coefficient does not increase as fast with increasing vertical field as the turbulent viscosity does. In Fig. 1 we plot the vertical and radial Schmidt numbers as a function of α. Both Schmidt numbers approximately follow a power law with α. Making a best-fitting power law, we find the empirical connections

$$\text{Sc}_x = 4.6\alpha^{0.26}, \tag{10}$$

$$\text{Sc}_z = 25.3\alpha^{0.46}. \tag{11}$$

Considering the two box sizes individually (black and grey symbols in Fig. 1), the radial Schmidt number is seen to rise slightly faster with increasing α in the case of the elongated box with $L_y = 4$, whereas the vertical Schmidt number follows a trend that is independent of the box size. In ideal magnetohydrodynamic simulations with $\beta = 400$, CSP05 find a radial Schmidt number of around 10. Using a similar value for β, we find that the radial Schmidt number rises from unity in the case of no external field to $\sim$3–4 when $\beta \simeq 400$. This may explain at least part of the discrepancy between the results by CSP05 and JK05. Th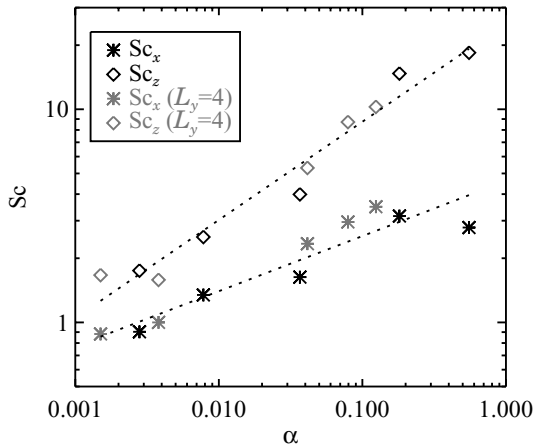e box size used in CSP05 is $1.0 \times$ 6.28×1.0, and is thus comparable to our elongated box. We have tried with $L_y = 6.28$ as well, but found no significant difference in the results.

It is interesting to note that Fromang & Papaloizou (2006) have an α-value of 0.015 and a vertical Schmidt number of 2.8. That fits almost perfectly in Fig. 1. Since Fromang & Papaloizou (2006) do not have an imposed vertical field in their simulations, this may mean that the rise in Schmidt number with α is something fundamental and not only an effect of the imposed magnetic field, although further investigations would have to be done to explore this connection in more detail.

4.1 Correlation times

One can express the diffusion coefficient caused by the scale k of a turbulent flow as $D_k = u_k \ell_k$. Here u_k is the velocity amplitude of that scale and ℓ_k is the typical length-scale over which a turbulent feature transports before dissolving. The advection length ℓ_k can be approximated by $\ell_k = u_k t_k$, where t_k is the correlation time, or life time, of a turbulent structure. Taking now an average (and weighted) correlation time τ_{cor} of all the scales, one gets the mixing length expression for the diffusion coefficient in direction i,

$$D_i^{(\text{t})} = \tau_{\text{cor}} u_i^2, \tag{12}$$

valid for Fickian diffusion [for the validity of Fickian diffusion see Brandenburg, Käpylä & Mohammed (2004)]. Here the Mach number, $\sqrt{u_i^2}/c_s$, is the root-mean-square velocity fluctuation in real space. The diffusion coefficient should thus scale roughly with Mach number squared. We plot the correlation times, calculated from equation (12), of δ_x and δ_z versus the α-value of the flow in Fig. 2. The correlation time of the turbulent diffusion coefficients falls steeply with increasing α-value, so even though the Mach number of the flow increases, the time that a given turbulent structure has for transporting the dust becomes shorter and shorter. Since the correlation times of radial and vertical diffusion have approximately the same dependence on α, the ratio of the diffusion coefficients can be expressed as $\delta_x/\delta_z = (\text{Ma}_x/\text{Ma}_z)^2$. The anisotropy in the diffusion coefficient in favour of the radial direction is then mostly an effect of the anisotropy between the radial and vertical Mach numbers.
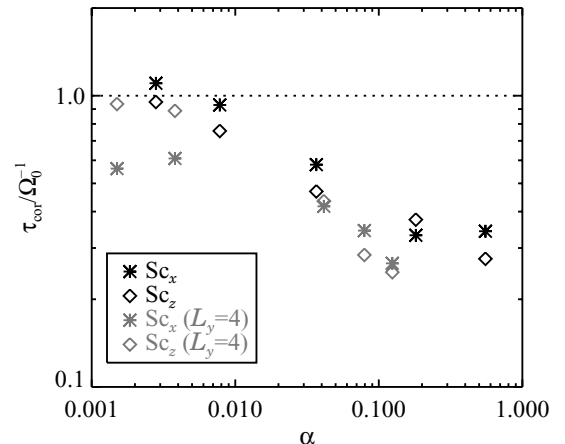

Figure 1. The Schmidt number plotted against the α-value and the best power-law fit (dotted lines). The best fit has $\text{Sc}_x = 4.6\,\alpha^{0.26}$ and $\text{Sc}_z = 25.3\alpha^{0.46}$.

Figure 2. The correlation time of the turbulent mixing coefficients versus the α-value. The correlation times fall significantly with increasing α.

5 SUMMARY

In this Letter we report that the Schmidt number of magnetorotational turbulence depends strongly on the value of an imposed vertical magnetic field. For large values of the vertical field, the relative strength of the turbulent diffusion falls with respect to the turbulent viscosity. This could explain part of the discrepancy between measurements of the radial turbulent diffusion coefficient in magnetorotational turbulence without an imposed field (Johansen & Klahr 2005) and with an imposed field (Carballido et al. 2005).

REFERENCES

Balbus S. A., Hawley J. F., 1991, ApJ, 376, 21
Barge P., Sommeria J., 1995, A&A, 295, L1
Bourke T. L., Myers P. C., Robinson G., Hyland A. R., 2001, ApJ, 554, 916
Brandenburg A., 2003, in Ferriz-Mas A., Núñez M., eds, The Fluid Mechanics of Astrophysics and Geophysics, Vol. 9, Advances in Nonlinear Dynamos. Taylor & Francis, London, p. 269
Brandenburg A., Nordlund Å., Stein R. F., Torkelsson U., 1995, ApJ, 446, 741
Brandenburg A., Käpylä P. J., Mohammed A., 2004, Phys. Fluids, 16, 1020
Camenzind M., 1990, Rev. Mod. Astron., 3, 234
Carballido A., Stone J. M., Pringle J. E., 2005, MNRAS, 358, 1055 (CSP05)
Dominik C., Blum J., Cuzzi J., Wurm G., 2006, in Reipurth B., Jewitt D., Keil K., eds, Protostars and Planets V, Univ. Arizona Press, Tucson, in press (astro-ph/0602617)
Dullemond C. P., Apai D., Walch S., 2006, ApJ, 640, L67
Fendt C., Elstner D., 1999, A&A, 349, L61
Fendt C., Elstner D., 2000, A&A, 363, 208
Fleming T., Stone J. M., 2003, ApJ, 585, 908
Fromang S., Papaloizou J., 2006, A&A, in press (astro-ph/0603153)
Gammie C. F., 1996, ApJ, 457, 355
Goldreich P., Tremaine S., 1978, ApJ, 222, 850
Goodman J., Xu G., 1994, ApJ, 432, 213
Haugen N. E. L., Brandenburg A., Mee A. J., 2004, MNRAS, 353, 94
Hawley J. F., Balbus S. A., 1992, ApJ, 400, 595
Hawley J. F., Gammie C. F., Balbus S. A., 1995, ApJ, 440, 742
Ilgner M., Nelson R. P., 2006, A&A, 445, 223
Ilgner M., Henning T., Markwick A. J., Millar T. J., 2004, A&A, 415, 643
Johansen A., Klahr H., 2005, ApJ, 634, 1353 (JK05)
Königl A., 1991, ApJ, 370, L39
Küker M., Henning T., Rüdiger G., 2003, ApJ, 589, 397
Miller K. A., Stone J. M., 1997, ApJ, 489, 890
Miller K. A., Stone J. M., 2000, ApJ, 534, 398
Rodmann J., Henning T., Chandler C. J., Mundy L. G., Wilner D. J., 2006, A&A, 446, 211
Sano T., Inutsuka S.-i., 2001, ApJ, 561, L179
Sano T., Inutsuka S.-i., Turner N. J., Stone J. M., 2004, ApJ, 605, 321
Semenov D., Wiebe D., Henning T. 2006, ApJ, submitted
Shakura N. I., Sunyaev R. A., 1973, A&A, 24, 337
Shu F., Najita J., Ostriker E., Wilkin F., Ruden S., Lizano S., 1994, ApJ, 429, 781
Steinacker A., Henning T., 2001, ApJ, 554, 514
Turner N. J., Willacy K., Bryden G., Yorke H. W., 2006, ApJ, 639, 1218
Vlemmings W. H. T., Diamond P. J., Imai H., 2006, Nat, 440, 58
Weidenschilling S. J., 1977, MNRAS, 180, 57
Willacy K., Langer W. D., Allen M., Bryden G., 2006, ApJ, in press (astro-ph/0603103)

This paper has been typeset from a TEX/LATEX file prepared by the author.